Time scales and relaxation dynamics in quantum-dot lasers

Thomas Erneux, Evgeny A. Viktorov, and Paul Mandel
Université Libre de Bruxelles, Optique Nonlinéaire Théorique, Campus Plaine, Code Postal 231, 1050 Bruxelles, Belgium
(Received 14 March 2007; published 21 August 2007)

We analyze a three-variable rate equation model that takes into account carrier capture and Pauli blocking in quantum dot semiconductor lasers. The exponential decay of the relaxation oscillations is analyzed from the linearized equations in terms of three key parameters that control the time scales of the laser. Depending on their relative values, we determine two distinct two-variable reductions of the rate equations in the limit of large capture rates. The first case leads to the rate equations for quantum well lasers, exhibiting relaxation oscillations dynamics. The second case corresponds to dots nearly saturated by the carriers and is characterized by the absence of relaxation oscillations.

DOI: 10.1103/PhysRevA.76.023819 PACS number(s): 42.55.Px, 42.60.Rn, 78.67.Hc

I. INTRODUCTION

After more than a decade of material development, quantum dot (QD) lasers are now a viable alternative to commercial quantum well (QW) lasers. QD edge-emitting lasers at 1300 nm on GaAs substrates exceed the performance of InP-based QW edge-emitters in several important factors such as threshold current, temperature stability, chirp, and feedback insensitivity [1,2]. They may thus find application in low-cost transmitter modules by releasing the need for temperature control, isolators, and external modulators. But the feasibility of high-speed transmission rates strongly depends on the damping rate of the relaxation oscillations (ROs) which inevitably appear in gain-switched operations [3]. Since 1997, the response of QD lasers have been systematically investigated through RO measurements [2,4,5] showing stronger damping than conventional QW lasers. These measurements used the expressions for the RO frequency and damping rate of QW lasers [6,7] and recent efforts have been directed to formulate more appropriate rate equations for QD lasers. The damped ROs observed experimentally in [8,9] have been simulated numerically using a five-variable rate equation model that incorporates microscopic kinetic equations and takes into account spontaneous emission. These equations are too complex for an analytical understanding of the QD unusual ROs and a simpler model describing the essential QD dynamical properties is desired. In QD semiconductor devices, the carriers are first injected into a wetting layer before being captured by a dot. In addition to the electrical field in the cavity and the carrier density in the wetting layer, we need to introduce the occupation probability of a dot and consider three rate equations that take into account the carrier capture process and Pauli blocking [10–12]. An alternative to the three-variable rate equation model is to modify the two-variable QW rate equations in a form suitable for QD lasers [15]. As we shall demonstrate, these two different approaches of the QD dynamical problem are not incompatible since two-variable models can be derived as asymptotic limits of the three-variable model. The two-variable QW rate equations indeed correspond to the limit of very large capture rates but a different limit is possible if the dots are nearly saturated by the carriers.

The objectives of this paper are twofold. First, we propose a first analytical explanation of the QD laser unusual relaxation properties. Second, we show that as a result of the multiple time scales of the QD laser, two quite different dynamical laser responses are possible depending on their design.

The rate equations formulated by O'Brien *et al.* [13] consist of three equations for the intensity I of the laser field in the cavity, the occupation probability ρ of a dot in the laser, and the number n of carriers in the wetting layer per dot. The dimensionless equations needed for an analytical study are formulated in Appendix A and are given by

$$I' = [-1 + g(2\rho - 1)]I, \tag{1}$$

$$\rho' = \eta[F(\rho,n) - \rho - (2\rho - 1)I], \tag{2}$$

$$n' = \eta[J - n - 2F(\rho,n)]. \tag{3}$$

The factor 2 in Eq. (3) accounts for the twofold spin degeneracy in the quantum dot energy levels. A similar factor 2 is included in the definition of the differential gain factor g in Eq. (1) [11]. The parameter $\eta = \gamma_n/\gamma_s \sim 10^{-3}$ is the ratio of the carrier and photon decay rates. The relaxation rates of ρ and n are assumed equal for mathematical simplicity. J is the pump current per dot and is the control parameter. The function $F(\rho,n)$ describes the carrier exchange rate between the wetting layer and the dots. In its most general form, the carrier exchange rate can be formulated as

$$F(\rho,n) = R^{\mathrm{cap}}(1-\rho) - R^{\mathrm{esc}}\rho, \tag{4}$$

where $1-\rho$ is the Pauli blocking factor, $R^{\mathrm{cap}} = Bn$ describes the carrier capture with rate $B \sim 10^3$, and R^{esc} describes the carrier escape from the dots to the wetting layer. At room temperature, $R^{\mathrm{esc}} \ll R^{\mathrm{cap}}$ and we shall ignore the escape process by setting $R^{\mathrm{esc}} = 0$. The three parameters B, η and $g-1$ control the time-dependent response of the QD laser. Since their precise values are difficult to evaluate experimentally, our objective is to derive analytical expressions for the damping rate valid for given range of values of B, η, and g. In the following sections, we consider η as our order parameter because it does not appear in the expressions of the steady states. We then scale B and $g-1$ with respect to η whenever it becomes necessary.

In order to investigate the damping of the relaxation oscillations, we consider the effect of a small perturbation from the nonzero intensity steady state. Its exponential decay can then be described in terms of the eigenvalues of the Jacobian matrix evaluated at the steady state. The characteristic equation for the growth rate is formulated in Sec. II. The basic approximation of the eigenvalues corresponding to the limit η small will be our starting point. In Sec. III, we examine the influence of B by scaling B with respect to η. Several cases are possible but one case emerges, giving a clear picture of the role of B from small to large values. Our results are tested numerically by simulating a turn-on experiment. Section IV examines a previous study of the RO growth rate. Finally, we discuss in Sec. V the combined role of the capture rate and the gain coefficient and derive two distinct two-variable models in the limit of large capture rates.

II. GROWTH RATES

From Eqs. (1)–(3), we first determine the steady states. In addition to the zero intensity solution, there exists a nonzero intensity steady state given by

$$\rho_s = \frac{1}{2}(1+g^{-1}), \tag{5}$$

$$n_s = \frac{J}{1+B_e}, \tag{6}$$

$$I_s = \frac{g}{2}\frac{B_e}{1+B_e}(J-J_{\mathrm{th}}) \tag{7}$$

where

$$J_{\mathrm{th}} \equiv \frac{1+B_e}{B_e}(1+g^{-1}) \text{ and } B_e \equiv B(1-g^{-1}) \tag{8}$$

are defined as the laser threshold pump current per dot and the effective capture rate, respectively. From the linearized equations, we then formulate the characteristic equation for the growth rate σ. It is mathematically more convenient to consider the steady state intensity I_s as the control parameter instead of J. This characteristic equation is

$$\sigma^3 + a_1\sigma^2 + a_2\sigma + a_3 = 0, \tag{9}$$

where

$$a_1 = \eta\left[1 + B_e + \frac{2(1+I_s)}{1-g^{-1}}\right], \tag{10}$$

$$a_2 = \eta\left[2I_s + \eta\frac{2(1+I_s)}{1-g^{-1}} + \eta B_e(1+2I_s)\right], \tag{11}$$

$$a_3 = 2I_s\eta^2(1+B_e). \tag{12}$$

Using the Routh-Hurwitz conditions [17], we find that the steady state is always stable. For the QW rate equations, the RO frequency is proportional to $\eta^{1/2}$ which motivates seeking a solution of Eq. (9) in power of $\eta^{1/2}$. Specifically, we introduce

$$\sigma = \eta^{1/2}\lambda_0 + \eta\lambda_1 + \cdots \tag{13}$$

into Eq. (9) and equate to zero the coefficients of each power of $\eta^{1/2}$. This leads to a series of linear problems for $\lambda_0, \lambda_1, \ldots$ In this way, we obtain

$$\sigma_{1,2} \simeq \pm i(2\eta I_s)^{1/2} - \eta\frac{1+I_s}{1-g^{-1}}, \tag{14}$$

$$\sigma_3 \simeq -\eta(1+B_e). \tag{15}$$

The imaginary part of the expression (14) gives the RO frequency

$$\Omega = (2\eta I_s)^{1/2}, \tag{16}$$

which is identical to the QW RO frequency. The real part of the expression (14) gives the damping rate

$$\Gamma_1 = \eta\frac{1+I_s}{1-g^{-1}}, \tag{17}$$

which differs from the QW damping rate given by

$$\Gamma_{\mathrm{QW}} = \frac{\eta}{2}(1+2I_s). \tag{18}$$

The expression (17) suggests that B does not have a strong effect since it only appears through I_s, given by Eq. (7), which remains $O(1)$ as $B \to \infty$. It is however important to realize that B cannot be too large since mathematically distinguished limits of the characteristic equation are possible if B scales like $\eta^{-1/2}$. This problem is analyzed in the next section.

III. LARGE CAPTURE RATE

Introducing $\sigma \equiv \eta^{1/2}\lambda$ into Eq. (9), the equation for λ is

$$\lambda^3 + b_1\lambda^2 + b_2\lambda + b_3 = 0, \tag{19}$$

where

$$b_1 = \eta^{1/2}\left[1 + B_e + \frac{2(1+I_s)}{1-g^{-1}}\right], \tag{20}$$

$$b_2 = 2I_s + \eta\frac{2(1+I_s)}{1-g^{-1}} + \eta B_e(1+2I_s), \tag{21}$$

$$b_3 = 2I_s\eta^{1/2}(1+B_e). \tag{22}$$

We wish to investigate the effect of large B. Because $I_s = I_s(B_e)$, we first need to expand I as a function of B_e^{-1}. Using its definition (7), we find that

$$I = I_0 + B_e^{-1}I_1 + \cdots, \tag{23}$$

where

$$I_0 = \frac{g}{2}[J - (1+g^{-1})] \quad \text{and} \quad I_1 = -\frac{g}{2}[J - 2(1+g^{-1})]. \tag{24}$$

We then note from the expressions (20) and (22) that B_e will contribute significantly to the characteristic equation only if $B_e = O(\eta^{-1/2})$. Introducing

$$B_e = \eta^{-1/2} B_1 \tag{25}$$

into Eq. (19) and seeking a solution of the form

$$\lambda = \lambda_0 + \eta^{1/2}\lambda_1 + \cdots , \tag{26}$$

we obtain a series of new problems for $\lambda_0, \lambda_1, \ldots$. The leading problem for λ_0 is

$$\lambda_0^3 + B_1\lambda_0^2 + 2I_0\lambda_0 + 2I_0 B_1 = 0, \tag{27}$$

which admits the solutions

$$\lambda_{01,02} = \pm i(2I_0)^{1/2}, \tag{28}$$

$$\lambda_{03} = -B_1. \tag{29}$$

The expression of the RO frequency provided by the solution (28) is identical to the expression (16) with $I_s = I_0$. To determine the RO damping rate, we investigate the next order problem for λ_1. This equation is given by

$$2\lambda_0\lambda_1(\lambda_0 + B_1) = \begin{bmatrix} -2I_1(\lambda_0 + B_1) - \left(1 + \dfrac{2(1+I_0)}{1-g^{-1}}\right)\lambda_0^2 \\ -B_1(1+2I_0)\lambda_0 - 2I_0 \end{bmatrix}, \tag{30}$$

where $\lambda_0 = \pm i(2I_0)^{1/2}$. Simplifying, we obtain

$$\mathrm{Re}(\lambda_1) = \frac{-1}{(2I_0 + B_1^2)}\left[\frac{(1+I_0)}{1-g^{-1}}2I_0 + \frac{B_1^2}{2}(1+2I_0)\right]. \tag{31}$$

Note that $\mathrm{Re}(\lambda_1) \to -\Gamma_1/\eta$ as $B_1 \to 0$, where Γ_1 is defined by (17). On the other hand, $\mathrm{Re}(\lambda_1) \to -\Gamma_{QW}/\eta$ as $B_1 \to \infty$, where Γ_{QW} is the QW damping rate (18). In Fig. 1, the new approximation $\Gamma_2 = \eta|\mathrm{Re}(\lambda_1)|$ is compared to the solution $\Gamma = |\mathrm{Re}(\sigma_{1,2})|$ obtained numerically from Eq. (9). We conclude that the damping rate decreases in the limit of very large B. But we also note from the first term in the right-hand side of the expression (31) that a value g close to 1 will contribute to an increase of the damping rate. We examine these two opposite effects in Secs. IV and V.

Next we propose to test the validity of our analytical predictions by simulating a turn-on experiment where the current J is changed from $J_- < J_{th}$ to $J_+ > J_{th}$. Specifically, we solve numerically Eqs. (1)–(3) with a constant $k = 10^{-4}$ added into the right-hand side of Eq. (1). This constant mimics the effect of noise by avoiding too small values of I during the turn-on process.

Figure 2 displays the influence of decreasing the capture rate B. Our analysis predicts an increase of the RO damping rate as we decrease B. This is indeed observed. Compared to Fig. 2(a), where $B = 1000$, Fig. 2(b), where $B = 100$, exhibits less RO oscillations.

Figure 3 investigates the effect of g. The analysis predicts that a decrease of $g-1$ contributes to an increase of the RO damping rate. Compared to Fig. 2(b), Fig. 3, where g is closer to 1, exhibits stronger damping. In the next section, we analyze the effect of g in detail.

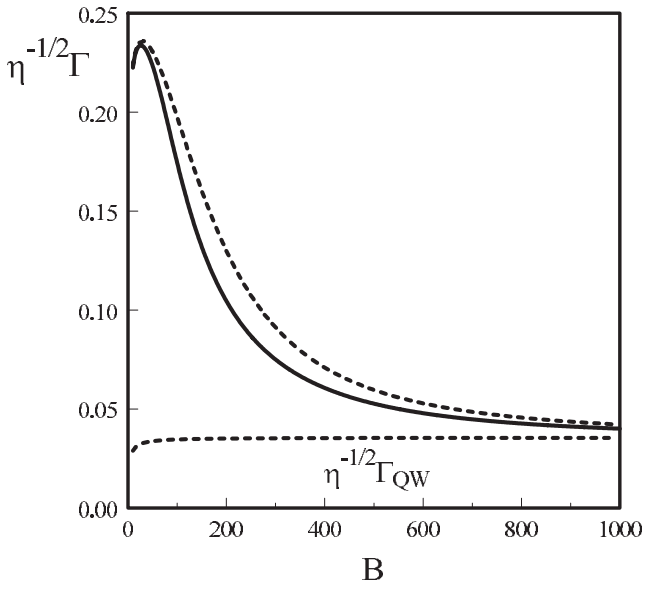

FIG. 1. Damping rate Γ as a function of B. $J - J_{th} = 1$, $\eta = 10^{-3}$, and $g = 1.25$. The full line represents $\Gamma = |\mathrm{Re}(\sigma_{1,2})|$ obtained numerically from Eq. (9). The upper broken line is the analytical approximation (31) where I_0 has been replaced by I_s to have a uniform expression valid for all I_s. The lower line is the approximation of the damping rate of the QW laser (18).

IV. THE EFFECT OF THE GAIN FACTOR

In [13], the damping rate is studied numerically as a function of the steady state dot occupation probability ρ_s defined by (5). Particular attention was devoted to the limit $\rho_s \to 1^-$ which is equivalent to the limit $g - 1 \to 0$. In order to be consistent with our previous asymptotic analysis with $B_e = O(\eta^{-1/2})$ and η small, we now need to specify how $g-1$ scales with η. From Eq. (19), we note that an interesting limit of the characteristic equation occurs if $B_e = \eta^{-1/2}B_1$ and $1 - g^{-1} = \eta^{1/2}c$. Since $B_e = B(1-g^{-1})$, this case is equivalent to

$$1 - g^{-1} = \eta^{1/2}c \text{ and } B = \eta^{-1}B_1. \tag{32}$$

Introducing the new parameters (32) and the expansion (26) into Eq. (19), we then find that $\lambda = \lambda_0$ satisfies the cubic equation

$$\lambda_0^3 + \left[B_1 c + \frac{2(1+I_0)}{c}\right]\lambda_0^2 + 2I_0\lambda_0 + 2I_0 B_1 c = 0 \tag{33}$$

that needs to be solved numerically [18]. The approximation of the damping rate $\Gamma_3 = \eta^{1/2}|\mathrm{Re}(\lambda_0)|$ is obtained from the real part of the complex-conjugate solutions of Eq. (33) and is represented as a function of ρ_s in Fig. 4 (curve b). We also represent in Fig. 4 the approximation $\Gamma_2 = \eta|\mathrm{Re}(\lambda_1)|$ where $\mathrm{Re}(\lambda_1)$ is given by the expression (31) (curve a) as well as the solution $\Gamma = |\mathrm{Re}(\sigma_{1,2})|$ obtained numerically from the original characteristic equation (9) (full line).

In the limit $c \to 0$, the complex solutions of Eq. (33) satisfy the quadratic equation

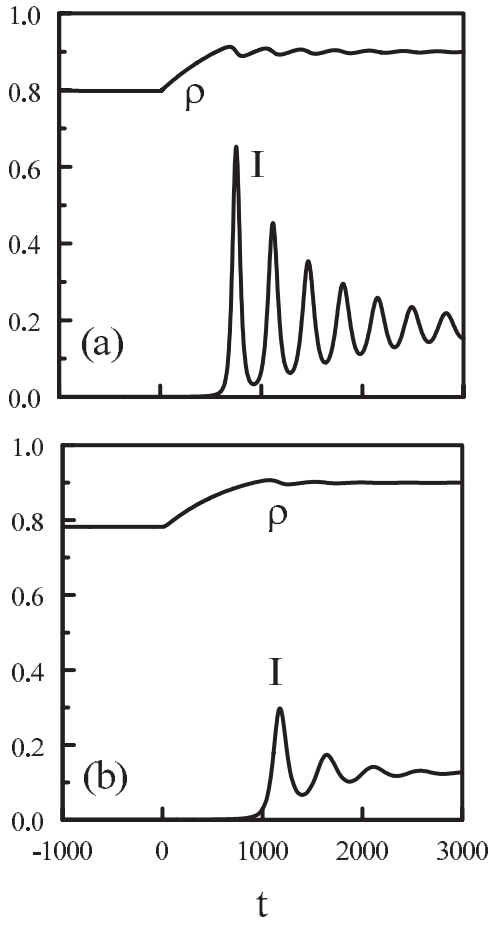

FIG. 2. Effect of B. The values of the fixed parameters are $\eta=10^{-3}$, $g=1.25$, $J_-=1.6$, and $J_+=2.1$. The laser is initially in its stable zero intensity steady state and $t=0$ corresponds to the abrupt change of J. (a) $B=1000$ and (b) $B=100$. All variables are dimensionless. Time is normalized by the photon lifetime.

$$\frac{2(1+I_0)}{c}\lambda_0^2 + 2I_0\lambda_0 + 2I_0B_1c = 0, \tag{34}$$

in first approximation. Solving Eq. (34) then leads to the complex solutions

$$\lambda_0 = \frac{c}{1+I_0}[-I_0 \pm 2i\sqrt{I_0^2(1-B_1) - 16I_0B_1}] \tag{35}$$

provided that $B_1 > I_0/(I_0+4)$. The growth rate is given by the real part and is proportional to $c=\eta^{-1/2}(1-g^{-1})$ (equivalently $1-\rho_s$), as anticipated analytically in [13]. The limit $c\to 0$ suggests the new case where the scaling (32) is replaced by

$$1 - g^{-1} = \eta d \text{ and } B = \eta^{-1}B_1. \tag{36}$$

We analyze this case in the next section.

V. LIMITS AND DISCUSSION

As long suspected, the capture rate of the carriers into empty dots contributes to the damping of the relaxation oscillations. In the limit of large effective capture rates [i.e., $B_e \equiv B(1-g^{-1}) \to \infty$], the RO damping rate Γ decreases and approaches the value Γ_{QW} of the QW laser. This may be understood as follows. If the capture rate is too large, the number of available carriers n will be small and the QD laser will behave like a conventional laser. On the other hand, we have shown that the QD damping rate is larger than the QW damping rate if $B_e=O(1)$. This can be realized even for large capture rates B provided that the deviation $g-1$ is small like B^{-1}. We then note from the expression (5) that the steady state occupation probability ρ_s is close to 1, meaning dot saturation. As a consequence, the carriers cannot be captured by dots and their number will be controlled only by the field in the cavity.

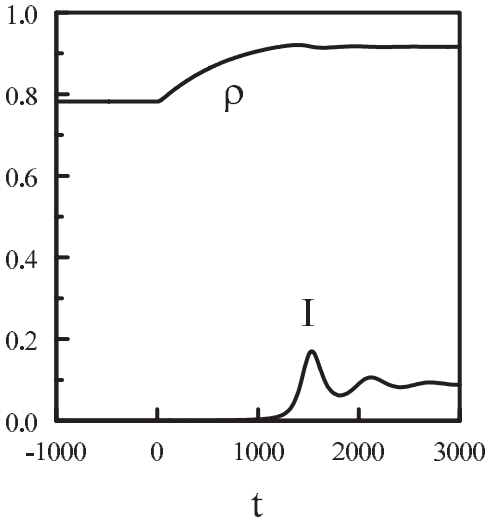

FIG. 3. Effect of g. The values of the fixed parameters are the same as in Fig. 2(b), i.e., $\eta=10^{-3}$, $J_-=1.6$, $J_+=2.1$, and $B=100$. Only the value of g has been reduced from 1.25 to 1.2. All variables are dimensionless. Time is normalized by the photon lifetime.

In order to clearly understand the combined effects of B large and $g-1$ small, we consider the large B limit of the full rate equations (1)–(3) and derive two distinct limits depending on g. As we shall now demonstrate, these two limits lead to the equations for a class B laser and a class A laser, respectively [16]. The first case is characterized by the decay rate of the carriers which is much smaller than the decay rate of the photons in the cavity. The second case is characterized by comparable time scales for both the photons and carriers.

The first case is defined by the scaling $B=O(\eta^{-1/2})$ and $g-1$ arbitrary and fixed. By introducing $n=B^{-1}\bar{n}$ into Eqs. (1)–(3), we note from the expression (3) that $\bar{n}$ can be eliminated adiabatically as

$$\bar{n} = \frac{J}{2(1-\rho)}. \tag{37}$$

The remaining equations for the gain $G \equiv g(2\rho-1)$ and I then become

$$I' = (-1+G)I, \tag{38}$$

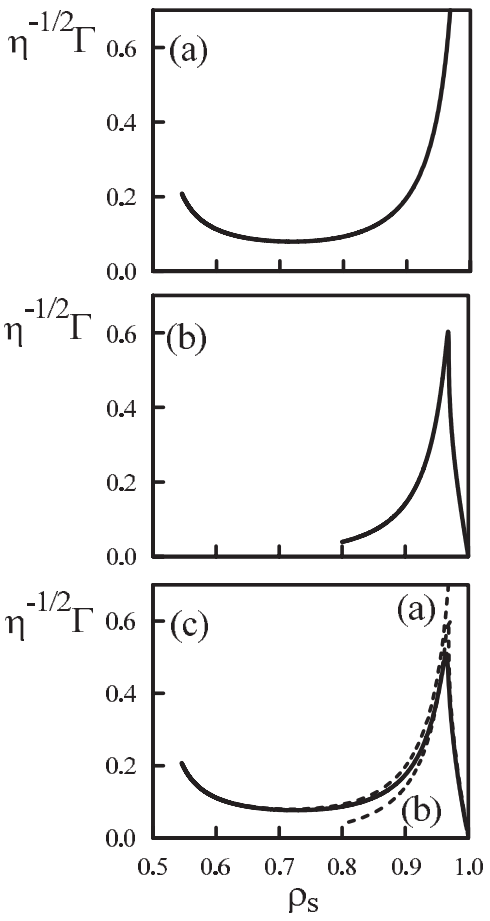

FIG. 4. The two approximations of the damping rate Γ. $\rho_s(g)$ is defined by (5) and g is changed from 1 to 10. $B=100$, $\eta=10^{-3}$, and $J-J_{\text{th}}=1$. (a) Analytical solution (31) valid for ρ_s not too close to 1. (b) Numerical solution of Eq. (33) valid for ρ_s close to 1. (c) Two approximations (a) and (b) (broken lines) are compared to the exact numerical solution (full line).

$$G' = \eta[J - g - G(1 + 2I)], \tag{39}$$

which we recognize as the QW laser rate equations.

The second case is defined by the scaling $B=O(\eta^{-1})$ and $g-1=O(\eta)$. We now consider the scaling (36), suggested by the analysis of the previous section. In addition to the scalings (36), we introduce the deviation $\rho=1-\eta\bar{\rho}$ and the new time
$s=\eta t$ into Eqs. (1)–(3). We then note that $\bar{\rho}$ can be eliminated adiabatically as

$$\bar{\rho} = \frac{1+I}{B_1 n} \tag{40}$$

and that the remaining equations for I and n reduce to

$$I' = \left[d - 2\frac{1+I}{B_1 n} \right] I, \tag{41}$$

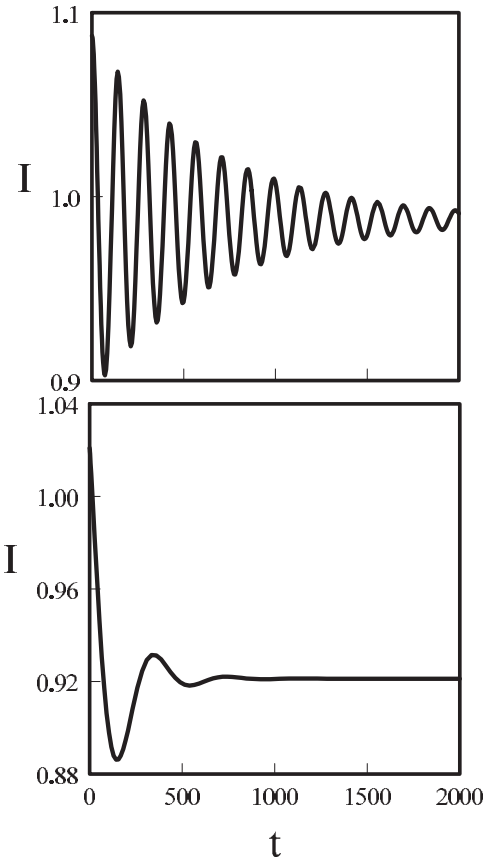

FIG. 5. Two-variable limits of the QD three-variable rate equations. Top: Solution of Eqs. (38) and (39) with $I(0)=I_s+0.1\simeq 1.09$ and $G(0)=G_s=1$. Bottom: Solution of Eqs. (41) and (42) with $I(0)=I_s+0.1\simeq 1.02$ and $n(0)=n_s\simeq 0.16$. The values of the fixed parameters are $g=1.025$, $B=10^3$, and $\eta=10^{-3}$. All variables are dimensionless. Time is normalized by the photon lifetime.

$$n' = J - n - 2(1 + I), \tag{42}$$

where prime means differentiation with respect to the time s. In this limit, the decay of the ROs occurs on the same time scale as the ROs. Figure 5 compare the evolution of the intensity for the two cases. The fixed parameters are identical and the perturbation of the steady state initiating the oscillatory decay is the same.

In summary, we have analyzed the decay of the ROs and discussed the role of the capture rate and the gain coefficient. Our analysis is based on a linearized theory and cannot anticipate the nonlinear response of the laser following an arbitrary perturbation of the steady state. Nevertheless, we may reasonably expect that the different scalings identified here will be useful for the analysis of the full nonlinear problem. This is illustrated in Appendix B where a nonlinear theory for the first case is derived.

ACKNOWLEDGMENTS

This work was inspired by many discussions over many years with the late Professor Lorenzo M. Narducci. This research was supported by the Fonds National de la Recherche

Scientifique (Belgium) and the Interuniversity Attraction Pole Programme-Belgian Science Policy.

APPENDIX A: DIMENSIONLESS RATE EQUATIONS

In QD semiconductor devices, the carriers are first injected into a wetting layer before being captured into a dot. Taking account this two-stage process, rate equations have been formulated by Sugawara *et al.* [10] and Uskov *et al.* [11] and further developed in [13,12]. In their simplest form, they consist of three coupled rate equations for the electrical field in the cavity, E, the number of carriers in the wetting layer per dot, N, and the occupation probability of a dot in the laser pumped with the current per dot J. In terms of the intensity $I=|E|^2$, these equations are

$$I' = -\gamma_s I + v_g g_0(2\rho - 1)I, \tag{A1}$$

$$\rho' = -\gamma_d \rho + CN(1-\rho) - v_g \sigma(2\rho - 1)I, \tag{A2}$$

$$N' = -\gamma_n N + J/q - 2CN(1-\rho). \tag{A3}$$

The rate of capture is described by the term $CN(1-\rho)$ and is proportional to the number of carriers present as well as the probability to find a dot. The parameters γ_n and γ_d represent non radiative decay rates, v_g is the group velocity and σ is the cross section of interaction of the carriers in a dot with the electrical field. γ_s is the photon decay rate in the cavity and g_0 is the differential gain. Introducing the dimensionless variables

$$t_1 \equiv \gamma_s t, \quad n = N, \text{ and } I_1 = \gamma_d^{-1} v_g \sigma I \tag{A4}$$

into Eqs. (A1)–(A3), we obtain

$$I_1' = [-1 + g(2\rho - 1)]I_1, \tag{A5}$$

$$\rho' = \eta_1[-\rho + Bn(1-\rho) - (2\rho - 1)I_1], \tag{A6}$$

$$n' = \eta[-n + J_1 - 2Bn(1-\rho)], \tag{A7}$$

where $\eta=\gamma_n/\gamma_s$, $\eta_1=\gamma_d/\gamma_s$, $g=\gamma_s^{-1}v_g g_0$, $J_1=\gamma_n^{-1}J/q$, and $B=\gamma_d^{-1}C$. Equations (A5)–(A7) are equivalent to Eqs. (1)–(3) with $F(\rho,n)=Bn(1-\rho)$. Moreover, t and I replace t_1 and I_1, respectively. Using the values of the parameters in [14], we determine $g=1.25$, $B=10^3$, and $\eta=\eta_1=3.3\times10^{-3}$. Note that larger values of B are possible since values of the capture time C^{-1} from 1 to 10^2 ps have been reported in the literature. With $\gamma_d=10^{-3}$ ps^{-1}, it gives $B=10-10^3$.

APPENDIX B: NONLINEAR THEORY FOR THE RO OSCILLATIONS

In this appendix, we take advantage of the scalings found in the linear stability analysis and formulate the nonlinear nearly conservative laser equations for the RO decaying oscillations. To this end, we introduce the deviations x, y, and z from the steady state defined as

$$I = I_s(1+y), \quad \rho = \rho_s + \delta x, \quad n = n_s + B^{-1}z, \tag{B1}$$

and the new time

$$s \equiv \omega t. \tag{B2}$$

The coefficients δ and ω are determined so that the small parameter η multiplying the right-hand side of Eq. (2) can be removed. We find $\omega\equiv\sqrt{2\eta I_s}$ and $\delta\equiv\omega/(2g)$. They are both $O(\eta^{1/2})$ small quantities. Inserting by the new variables (B1) and (B2) into Eqs. (1)–(3), we obtain

$$x' = \left[-y + z\frac{g}{2I_s}(1-g^{-1}) - \frac{g\delta x}{I_s}[Bn_s + z + 1 + 2I_s(1+y)]\right], \tag{B3}$$

$$y' = (1+y)x, \tag{B4}$$

$$z' = \frac{B\eta}{\omega}[-z(1-g^{-1}) - B^{-1}z + 2\delta x(Bn_s + z)], \tag{B5}$$

where prime now means differentiation with respect to time s. We next assume that $B=O(\eta^{-1/2})$ and analyze the limit $\eta\to0$ of these equations. The leading order equation for z is linear which means that we may determine the solution of Eq. (B5) by a regular perturbation series in δ. The solution in its simplest form $[z(0)=0]$, and after using $Bn_s=J/(1-g^{-1})+O(B^{-1})$, is given by

$$z = \frac{B\eta J}{g-1}\exp(-Es)\int_0^s \exp(Es)x(s)ds + O(\eta), \tag{B6}$$

where $E\equiv(B\eta/\omega)(1-g^{-1}+B^{-1})$. Introducing $u=\ln(1+y)$, Eqs. (B3) and (B4) with the expresssion (B6) can be reformulated as a weakly perturbed second order differential equation for u of the form

$$u'' - 1 + \exp(u) = -\delta\frac{gu'}{I_s}\left(\frac{J}{1-g^{-1}} + 1 + 2I_s\exp(u)\right) + B\eta\frac{J}{2I_s}\exp(-Es)\int_0^s \times\exp(Es)u'(s)ds + O(\eta). \tag{B7}$$

The left-hand side is a Toda equation for the laser conservative oscillations [19]. The right-hand side contains two main contributions. The first term multiplying δ represents the usual damping of the class B laser RO oscillations. The second term multiplying $B\eta$ is an integral term and represents the effect of the relaxation of the carriers in the wetting layer.

[1] D. Bimberg, M. Grundmann, and N. N. Ledentsov, *Quantum Dot Heterostructures* (Wiley, New York, 1999).
[2] M. Kuntz, N. N. Ledentsov, D. Bimberg, A. R. Kovsh, V. M. Ustinov, A. E. Zhukov, and Y. M. Shernyakov, Appl. Phys. Lett. **81**, 3846 (2002).
[3] Systematic studies of laser dynamical responses started in the early eighties. See feature issue on "Instabilities in Active Optical Media," edited by N. B. Abraham, L. A. Lugiato, and L. M. Narducci, J. Opt. Soc. Am. A **2**(1) (1985).
[4] M.-H. Mao, F. Heinrichsdorff, A. Krost, and D. Bimberg, Electron. Lett. **33**, 1641 (1997).
[5] M.-H. Mao, T.-Y. Wu, D.-C. Wu, F.-Y. Chang, and H.-H. Lin, Opt. Quantum Electron. **36**, 927 (2004).
[6] G. P. Agrawal and N. K. Dutta, *Long-Wavelength Semiconductor Lasers* (Van Nostrand Reinhold, New York, 1986).
[7] K. Petermann, *Laser Diode Modulation and Noise* (Kluwer Academic, Dordrecht, The Netherlands, 1988) (reprinted 1991).
[8] E. Malic, K. J. Ahn, M. J. P. Bormann, P. Hovel, E. Scholl, A. Knorr, M. Kuntz, and D. Bimberg, Appl. Phys. Lett. **89**, 101107 (2006).
[9] E. Malic, M. Bormann, P. Hövel, M. Kuntz, D. Bimberg, E. Schöll, and A. Knorr (unpublished).
[10] M. Sugawara, K. Mukai, and H. Shoji, Appl. Phys. Lett. **71**, 2791 (1997).
[11] A. V. Uskov, Y. Boucher, J. Le Bihan, and J. McInerney, Appl. Phys. Lett. **73**, 1499 (1998).
[12] M. Ishida, N. Hatori, T. Akiyama, K. Otsubo, Y. Nakata, H. Ebe, M. Sugawara, and Y. Arakawa, Appl. Phys. Lett. **85**, 4145 (2004).
[13] D. O'Brien, S. P. Hegarty, G. Huyet, and A. V. Uskov, Opt. Lett. **29**, 1074 (2004).
[14] S. Melnik, G. Huyet, and A. V. Uskov, Opt. Express **14**, 2950 (2006).
[15] A. Fiore and A. Markus, IEEE J. Quantum Electron. **43**, 287 (2007).
[16] J. R. Tredicce, F. T. Arecchi, G. L. Lippi, and G. P. Puccioni, J. Opt. Soc. Am. B **2**, 173 (1985).
[17] J. V. Uspensky, *Theory of Equations* (McGraw-Hill, New York, 1948).
[18] In [13], the authors used $R^{\mathrm{cap}}=CN^2$ instead of $R^{\mathrm{cap}}=BN$ but the qualitative behavior of the damping rate with its two extrema is similar for both cases.
[19] G. L. Oppo and A. Politi, Z. Phys. B: Condens. Matter **59**, 111 (1985).